

Evaluation of a 4-Protein Serum Biomarker Panel—Biglycan, Annexin-A6, Myeloperoxidase, and Protein S100-A9 (B-AMP)—for the Detection of Esophageal Adenocarcinoma

Ali H. Zaidi, MD¹; Vanathi Gopalakrishnan, PhD²; Pashtoon M. Kasi, MD³; Xuemei Zeng, PhD⁴; Usha Malhotra, MD⁵; Jeya Balasubramanian, MS²; Shyam Visweswaran, MD, PhD²; Mai Sun, MS⁴; Melanie S. Flint, PhD⁴; Jon M. Davison, MD⁴; Brian L. Hood, PhD⁴; Thomas P. Conrads, PhD⁴; Jacques J. Bergman, MD, PhD⁶; William L. Bigbee, PhD⁴; and Blair A. Jobe, MD, FACS¹

BACKGROUND: Esophageal adenocarcinoma (EAC) is associated with a dismal prognosis. The identification of cancer biomarkers can advance the possibility for early detection and better monitoring of tumor progression and/or response to therapy. The authors present results from the development of a serum-based, 4-protein (biglycan, myeloperoxidase, annexin-A6, and protein S100-A9) biomarker panel for EAC. **METHODS:** A vertically integrated, proteomics-based biomarker discovery approach was used to identify candidate serum biomarkers for the detection of EAC. Liquid chromatography-tandem mass spectrometry analysis was performed on formalin-fixed, paraffin-embedded tissue samples that were collected from across the Barrett esophagus (BE)-EAC disease spectrum. The mass spectrometry-based spectral count data were used to guide the selection of candidate serum biomarkers. Then, the serum enzyme-linked immunosorbent assay data were validated in an independent cohort and were used to develop a multiparametric risk-assessment model to predict the presence of disease. **RESULTS:** With a minimum threshold of 10 spectral counts, 351 proteins were identified as differentially abundant along the spectrum of Barrett esophagus, high-grade dysplasia, and EAC ($P < .05$). Eleven proteins from this data set were then tested using enzyme-linked immunosorbent assays in serum samples, of which 5 proteins were significantly elevated in abundance among patients who had EAC compared with normal controls, which mirrored trends across the disease spectrum present in the tissue data. By using serum data, a Bayesian rule-learning predictive model with 4 biomarkers was developed to accurately classify disease class; the cross-validation results for the merged data set yielded accuracy of 87% and an area under the receiver operating characteristic curve of 93%. **CONCLUSIONS:** Serum biomarkers hold significant promise for the early, noninvasive detection of EAC. *Cancer* 2014;120:3902-13. © 2014 American Cancer Society.

KEYWORDS: esophageal adenocarcinoma, biomarker, serum, early detection, monitoring, protein.

INTRODUCTION

The incidence of esophageal adenocarcinoma (EAC) is rapidly rising, outpacing the rates of increase for all other cancers. The number of patients affected per year is up to 600% higher than it was in the 1970s.^{1,2} In addition, EAC is associated with a dismal prognosis, with a 5-year survival rate $< 15\%$. Although survival and prognosis depend on the stage of the disease, unfortunately, because the esophagus is a distensible organ, the majority of patients who develop EAC do not sense difficulty swallowing until the tumor is advanced.³ Accordingly, there is an urgent need for improved risk stratification to facilitate early detection and thereby reduce mortality from EAC.⁴

Currently, without clinical risk factors that signal the early development of EAC, the identification of early stage and curable disease is only possible through endoscopic Barrett esophagus (BE) screening for patients who have symptoms of gastroesophageal reflux disease (GERD).^{5,6} Those diagnosed with BE then typically undergo lifetime endoscopic surveillance for the development of malignancy.⁷ However, 95% of patients who develop EAC have never undergone BE screening before their cancer diagnosis, and up to 57% of patients who develop EAC do not report antecedent GERD symptoms.^{8,9}

The identification of cancer biomarkers raises the possibility for early detection and for better monitoring of tumor progression and/or response to therapy. Protein biomarkers that have been identified and are in regular clinical use for

Corresponding author: Blair A. Jobe, MD, FACS, Director, Institute for the Treatment of Esophageal and Thoracic Disease, Allegheny Health Network, 4600 North Tower, 4800 Friendship Avenue, Pittsburgh, PA 15224; Fax: (412) 578-1434; bjobe1@wpahs.org

¹Institute for the Treatment of Esophageal and Thoracic Disease, Allegheny Health Network, Pittsburgh, Pennsylvania; ²Department of Biomedical Informatics, University of Pittsburgh, Pittsburgh, Pennsylvania; ³International Scholars Program, Department of Medicine, University of Pittsburgh Medical Center, Pittsburgh, Pennsylvania; ⁴University of Pittsburgh Cancer Institute, University of Pittsburgh, Pittsburgh, Pennsylvania; ⁵Department of Medicine, Roswell Park Cancer Institute, Buffalo, New York; ⁶Department of Gastroenterology and Hepatology, Academic Medical Center, Amsterdam, Netherlands.

DOI: 10.1002/cncr.28963, **Received:** May 20, 2014; **Revised:** June 23, 2014; **Accepted:** July 22, 2014, **Published online** August 5, 2014 in Wiley Online Library (wileyonlinelibrary.com)

different tumors include carcinoembryonic antigen, prostate-specific antigen, α -fetoprotein, and cancer antigen 125. The development of biomarkers is even more important for cancers like EAC, which typically are diagnosed at an advanced disease stage and have poor long-term survival rates with the currently used clinical management paradigm.¹⁰

Toward this goal, in the current report, we present results from a serum-based, 4-protein biomarker panel for EAC (comprising biglycan [BGN], annexin-A6 [ANXA6], myeloperoxidase [MPO], and protein S100-A9 [S100A9] [B-AMP]) that was identified using a vertically integrated, proteomics-based biomarker discovery approach initially to identify candidate tissue and then to identify serum biomarkers. We observed that these proteins were clinically relevant and followed a distinct pattern of expression along the sequence of disease progression. These data were subsequently used to develop a multiparametric risk-assessment model for predicting the presence of disease.

MATERIALS AND METHODS

Figure 1 outlines the overall study schema, including patient populations and the methods used. This study was initiated in 2009 and completed in 2013. Institutional Review Board approval was obtained before the initiation of the study, and informed consent was obtained at the time of tissue collection.

Proteomic Biomarker Identification From BE, High-Grade Dysplasia, and EAC Tissues

To identify candidate protein biomarkers associated with disease progression, we performed a mass spectrometry-based proteomics discovery study using appropriate pathologically defined esophageal tissue specimens. The tissue discovery data were generated from archival deidentified, formalin-fixed, paraffin-embedded (FFPE) blocks obtained from the Department of Pathology at the University of Pittsburgh. This cohort consisted of 10 samples of BE, 11 samples of high-grade dysplasia (HGD) and 10 unpaired patient samples of advanced locoregional EAC (see Fig. 1; tissue discovery cohort).

A single-tube experimental protocol was used to digest proteins from FFPE tissue sections with trypsin, and the resultant tryptic peptides were analyzed using liquid chromatography-tandem mass spectrometry (LC-MS/MS) for an exploratory proteomic analysis of BE, HGD, and EAC. Approximately 40,000 cells per sample were collected by laser-capture microdissection (LCM); the tryptic digests were analyzed in duplicate by nanoflow

LC-MS/MS using a hybrid linear ion trap-orbitrap mass spectrometer. The primary MS/MS data were searched with the SEQUEST data-analysis program (ThermoFisher Scientific Inc., Waltham, Mass) against the human proteome database for peptide identification and against a “decoy” human proteome database in which the protein sequences are reversed to maintain a false-discovery rate <1%.¹¹ Next, we integrated the resulting peptide lists using a suite of in-house, MATLAB-enabled relational database tools (The MathWorks, Natick, Mass) to yield spectral counts for the identified proteins.

A quantitative estimate of the relative abundance of the identified proteins from these data sets was obtained by comparison of their spectral count values between BE-derived, HGD-derived, and EAC-derived cells. To determine statistically significant, differentially abundant proteins from each tissue type, we applied a Kruskal-Wallis nonparametric analysis of variance test (the Kruskal-Wallis test is a 1-way analysis of variance by ranks and determines statistically significant differences between 2 or more groups of an independent variable on a continuous or ordinal, dependent variable); proteins with significant differences were used for further hierarchical clustering analysis.

Digestion of LCM FFPE Tissues

Heat-induced trypsin digestion was applied to the LCM cells to extract peptides as previously described.¹² Samples were resuspended in 100 μ L of 100 mM NH_4HCO_3 /20% acetonitrile, then heated at 90°C for 1 hour, and stored at 65°C for 2 hours. Trypsin digestion was carried out by adding 500 ng of sequencing grade, modified trypsin (Promega, Madison, Wis) followed by an overnight incubation at 37°C. After a rapid spin, the aqueous solution was transferred to a new Eppendorf tube, lyophilized, and then resuspended in 100 μ L 0.1% trifluoroacetic acid (TFA), followed by desalting with PepClean C-18 Spin Columns (Pierce, Rockford, Ill), vacuum drying, and resuspension in 25 μ L 0.1% TFA. The BCA assay (Pierce) was used to determine peptide concentrations.

LC-MS/MS Analysis of Peptides

The tryptic digests were analyzed in duplicate (1 μ g for each injection) by reverse-phase LC-MS/MS using a nanoflow LC system (Dionex Ultimate 3000; Dionex Corporation, Sunnyvale, Calif) coupled online to an LTQ/Orbitrap XL hybrid mass spectrometer (ThermoFisher Scientific Inc., San Jose, Calif). Peptide separation was performed using fused silica capillary columns (75- μ m inner diameter \times 360- μ m outer diameter \times 20-cm

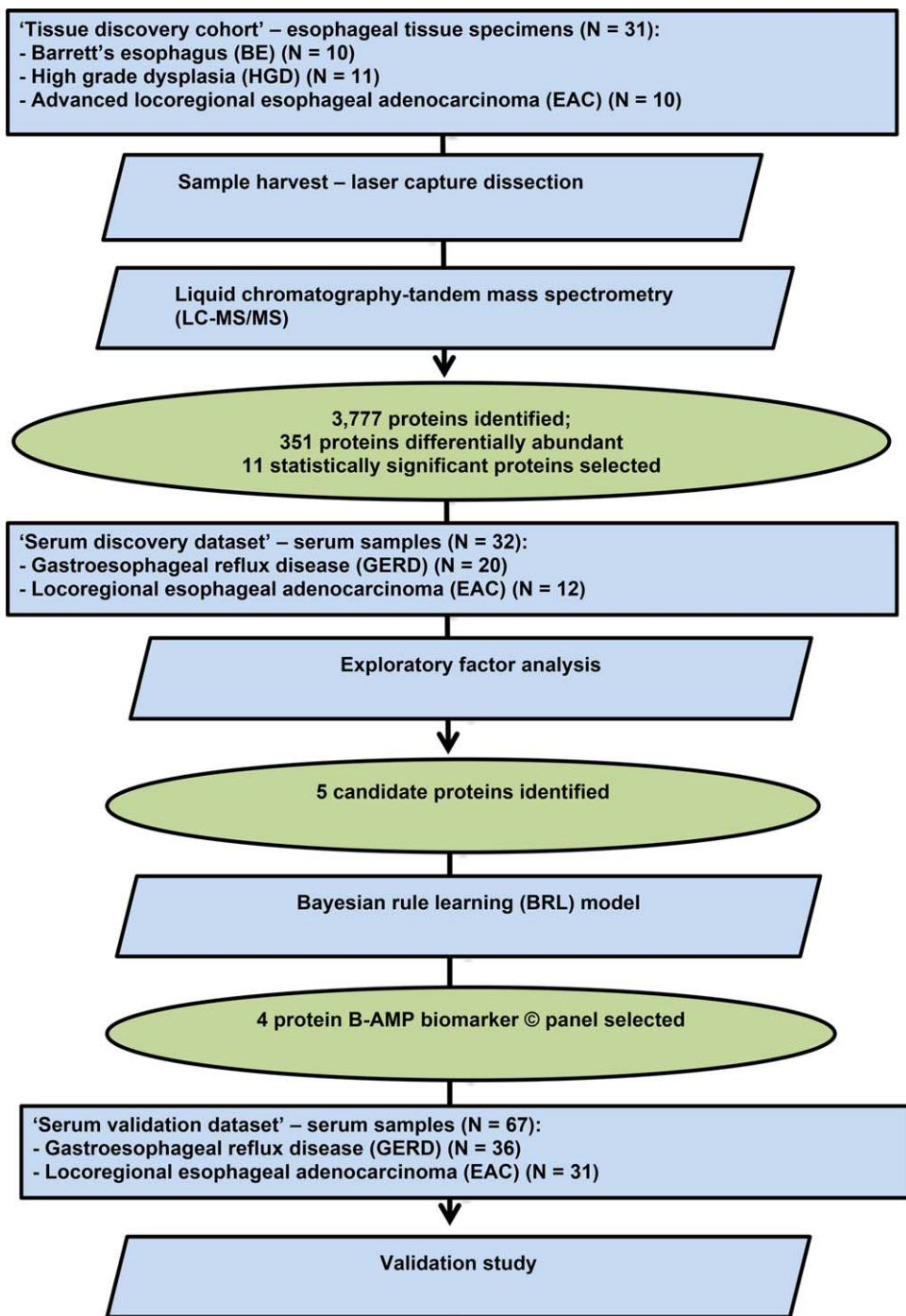


Figure 1. The study schema is illustrated with the patient populations and methods used. Serum protein biomarker discovery was guided by tissue-based proteomics followed by analysis and evaluation in serum samples using enzyme-linked immunosorbent assays.

long; Polymicro Technologies, Phoenix, Ariz), which were slurry packed in-house with 5- μ m, 300-angstrom pore size C-18 silica-bonded stationary phase (Jupiter; Phenomenex, Torrance, Calif). After sample injection onto a C-18 trap column (Dionex Corporation), the col-

umn was washed for 3 minutes with mobile phase A (2% acetonitrile, 0.1% formic acid) at a flow rate of 30 μ L per minute. Peptides were eluted using a linear gradient of 0.30% mobile phase B (0.1% formic acid in acetonitrile) per minute for 130 minutes, then to 95% B for an

additional 10 minutes, all at a constant flow rate of 250 nL per minute. Column washing was performed at 95% mobile phase B for 20 minutes, after which the column was re-equilibrated in mobile phase A before subsequent injections. The LTQ/Orbitrap XL mass spectrometer was configured to collect high-resolution ($R=60,000$ at a mass-to-charge [m/z] ratio of 400) broadband mass spectra (m/z ratio, 375-1800) from which the 7 most abundant peptide molecular ions dynamically determined from the mass spectrometry scan were selected for MS/MS using a 30% normalized, collision-induced dissociation energy. Dynamic exclusion was used to minimize redundant selection of peptides for MS/MS analysis.

Mass Spectrometry and MS/MS Data Analysis

For relative quantification using spectral count, tandem mass spectra were searched against the UniProt human proteome database (June 2009 release) from the European Bioinformatics Institute (available at: <http://www.ebi.ac.uk/integr8>; accessed November 8, 2010) using SEQUEST (ThermoFisher Scientific Inc.) with variable modification of methionine (oxidation, +15.9949 Da). The mass tolerance for the precursor ions and fragment ions were set to 20 ppm and 1 Da, respectively. Peptides were considered legitimately identified if they achieved specific charge state and proteolytic cleavage-dependent cross-correlation (Xcorr) scores of 1.9 for $[M+H]^1+$, 2.2 for $[M+2H]^2+$, and 3.5 for $[M+3H]^3+$, and a minimum delta correlation score (ΔCn) of 0.08. An in-house MATLAB script was used to combine the total number of collision-induced dissociation spectra that resulted in positive identification of any peptides for a given protein (spectral count).

Hierarchical clustering was carried out using MATLAB (The MathWorks). The values for spectral counts were standardized for each protein so that each had a mean of 0 and a standard deviation of 1. Both sample distance and protein feature distance were calculated using Pearson correlation, and average linkage was used for the clustering of both samples and protein features.

Patient Study Populations and Serum Sample Collection, Processing, and Storage

For an initial evaluation of the abundances of the candidate protein biomarkers in serum, a *serum discovery data set* of samples was collected from a total of 32 patients, including 20 patients who had a clinical diagnosis of GERD and 12 patients who had advanced, locoregional EAC (T2N1 to T3N0) from the Esophageal Risk Registry at the University of Pittsburgh in 2010.

For this purpose, venous blood samples (4 mL) from normal controls with GERD and patients with EAC were drawn using standard venipuncture into red/yellow-top Vacuette Serum Clot Activator with Gel Separator blood collection tubes (catalog no. 454067; Greiner-Bio-One, Monroe, NC) and were placed upright for 30 to 60 minutes until clot formation. The tubes were centrifuged in a swinging bucket rotor ($\times 1300g$ for 20 minutes), and the serum was pipetted and distributed as 200- μ L aliquots into 1.5-mL cryovials for storage at -80°C . To ensure consistency and reliability in the subsequent analyses, no more than 1 freeze-thaw cycle was allowed for any sample.

Enzyme-Linked Immunosorbent Assay Testing for the Candidate Serum Protein Biomarker Panel

Commercial enzyme-linked immunosorbent assay (ELISA) kits were used to quantify the abundance of the candidate biomarkers in serum (Supporting Table 1; see online supporting materials). The following ELISA kits were used: alpha-1-antitrypsin (A1A), myeloperoxidase (MPO), and apolipoprotein A-I (APO A1) (catalog no. E-80A, E-80PX, and E80AP1, respectively; Immunology Consultants Laboratory, Inc., Portland, Ore); resistin (catalog no. DRSN00; R&D Systems, Minneapolis, Minn); isoform 1 of fibronectin (catalog no. EF1045; Bioxys, Brussels, Belgium); lymphocyte cytosolic protein 1 (LCP1) (catalog no. ABIN415176; Antibodies-Online.com, Atlanta, Ga); Cathespin B (catalog no. SEC964Hu; USCNK Life Science Inc., Wuhan, China); protein S-100A9/MRP14, biglycan, and annexin A6 (catalog no. CY-8062, SE9822HU, SE92345HU, respectively; CedarLane, Burlington, NC); and cellular fibronectin (catalog no. 6030010; Biohit, Helsinki, Finland). Briefly, each assay comprised a singleplex, sandwich ELISA with primary antibody specific for the selected protein precoated in planar arrays in 96-well microtiter plates. After serum incubation and washing, a second biotinylated antibody to a different site on the protein from the capture epitope was introduced, and streptavidin-horseradish peroxidase subsequently bound to the biotinylated detection antibody. Chromogen-substrate reagent was added, and the absorbance (optical density) was read according to the manufacturer's instructions on a Spectra-Max M2e plate reader (Molecular Devices, Sunnyvale, Calif). The optical density values were acquired and processed using a 4-parameter curve fit to compare the experimental samples with the recombinant protein calibration curve run in parallel wells to derive absolute protein concentrations adjusted for dilution.

Validation Study of the Selected Serum Biomarkers

A second-stage study of 67 independent serum samples (*serum validation data set*) from 36 non-BE controls with GERD and 31 patients with EAC from Roswell Park Cancer Institute and the Allegheny Health Network was conducted to validate the previous findings in the 32-sample *serum discovery data set* from patients at the University of Pittsburgh. The sample-preparation and quality-control protocols and serum ELISAs were performed as described above for the serum discovery data set using the final 5 candidate biomarkers that demonstrated statistical discrimination between the 2 patient groups in the initial data set.

Development of a Serum Biomarker Panel and Predictive Model for EAC

Serum ELISA data from the discovery and validation data sets were subsequently used to develop and test predictive biomarker rule models using a new bioinformatics method called the Bayesian rule-learning (BRL) system.¹³ The BRL is a set of classification algorithms that we previously applied successfully to biomarker discovery and validation from serum proteomic data sets for the early detection of amyotrophic lateral sclerosis and lung cancer.^{14,15}

A rule model consists of a set of “IF-THEN” rules. For example: *IF (BGN>245 μg/mL) AND (S100A9>3 ng/mL) AND (MPO>120 ng/mL) THEN (class=EAC); posterior probability=.917, P=.0, true-positive=21, false-positive=1.*

This rule states that, if a patient sample has the biomarkers BGN, S100-A9, and MPO with serum levels >245 μg/mL, >3 ng/mL, and >120 ng/mL, respectively (defined in the IF part of the rule), then the patient has EAC (defined in the THEN part of the rule). The posterior probability indicates the probability of a true-positive result for EAC given all positive matches from the rule. The *P* value (*P*) of the rule is obtained from the Fisher exact test,¹⁶ which is a significance test appropriate for categorical count data such as the number of true-positive results and the number of positive results corresponding to each rule.

First, the BRL system learns a Bayesian network¹⁷ constrained to the target node (EAC or non-EAC); subsequently, biomarkers are added as potential parents to that node. The system learns the Bayesian network from the training data and evaluates it using an extension of the K2 score,^{13,18} assuming all models are equally probable a priori (uniform prior distribution). Details of the BRL algo-

gorithms have been published by Lustgarten and colleagues.^{13,18,19}

Because the BRL method can handle only discrete variables, we discretized the continuous-valued ELISA data for each biomarker into a small number of intervals using a method we have developed called efficient Bayesian discretization (EBD).²⁰ For each biomarker, EBD identifies a small number of intervals in the range of values for that biomarker that is optimal in terms of a Bayesian measure (based on the K2 score¹⁸). It has been demonstrated that using EBD to discretize variables yields better classification performance on a range of biomedical data sets.²¹

We generated predictive rule models from the *discovery data set* and applied them to the *validation data set* using different values for the user-defined λ parameter, which is the mean of a Poisson distribution that represents the expected number of cutoff points between the ranges of continuous values for each biomarker. We observed that λ values of 0.5 and 1.0 yielded models with the highest predictive accuracies. To use the validation data as a test set for predictive rule models, first, it was necessary to normalize the quantities for each biomarker in the discovery and validation data sets together using Equation (1).

$$F = \frac{\frac{1}{N_+(D_T)} \sum_{p=1}^{N_+(D_T)} D_T^p}{\frac{1}{N_-(D_V)} \sum_{q=1}^{N_-(D_V)} D_V^q} \quad (1)$$

Here, *F* is the factor of normalization computed for each biomarker, and N_+ and N_- refer to the total number of cases and controls, respectively, in each of the data sets: training (D_T) and test (D_V), respectively. The variables *p* and *q* iterate over instances with a specific class value (EAC or non-EAC) in the training data set (*p*) and the validation data set (*q*), respectively.

With the normalized data set values as determined above, we generated predictive rules from the discovery and validation data sets using each 1 independently as the training data set and the test data set, respectively. We further appended the discovery and validation data sets to create a merged data set to which we then applied 10-fold stratified cross-validation. Herein, we randomized and divided the combined data set into 10 almost equal portions. Then, we learned a predictive model from 9 portions of the data, designated as *training data*, and tested the remaining set-aside portion. This was done 10 times by applying BRL to learn a predictive model over each fold and testing that model to obtain performance metrics. Finally, average accuracy, balanced accuracy (BACC) (average of sensitivity and specificity), and area

under the receiver operating characteristic curve (AUROC) metrics were reported over this 10-fold cross-fold validation. To develop the final predictive model that we report here, we applied BRL to the complete merged data set.

Sample Size and Statistical Analysis

The serum validation study required 26 patients per group for an anticipated effect size of 0.8 with a calculated study power of 80% and a target α of .05. Statistical analyses were performed using SPSS software, version 20 (IBM Corporation, Armonk, NY). A P value $<.05$ was considered statistically significant.

RESULTS

Tissue-Based LC-MS/MS Proteomics Biomarker Identification

In total, 3777 proteins were identified from 62 LC-MS/MS analyses (duplicate analyses for each of the 31 tissue samples). The range of total spectral counts obtained in each sample analysis ranged from 2759 to 5181 and was significantly associated with the patient groups (Kruskal-Wallis test; $P=.0364$). With a minimum threshold of 10 spectral counts, we observed that 351 proteins were differentially abundant along the spectrum of BE, HGD, and EAC (Kruskal-Wallis test; $P<.05$) (Fig. 2, Supporting Table 1 [see online supporting materials]). These results indicated nearly perfect clustering of relative protein abundance from BE to EAC (Fig. 2).

B-AMP Biomarker ELISA

Eleven of the 351 differentially abundant proteins were selected for evaluation in serum using ELISAs on discovery sample sets based on their functional relevance and the availability of commercial ELISA kits. The serum ELISA results obtained from these selected tissue-based candidate biomarkers demonstrated significantly elevated serum levels for 5 of the 11 proteins tested in the EAC patient samples compared with the non-BE GERD samples in the serum discovery data set (Fig. 3). These included ANXA6, BGN, S100A9, MPO, and resistin. The serum levels followed similar trends across the disease spectrum, as observed in the corresponding tissue samples (Table 1, Fig. 1).

Table 1 summarizes the observed differences in candidate biomarker protein abundance measured by LC-MS/MS and spectral counting along the disease spectrum in FFPE-derived tissue samples and their corresponding concentrations in serum samples determined by ELISA. Largely consistent with the results in the se-

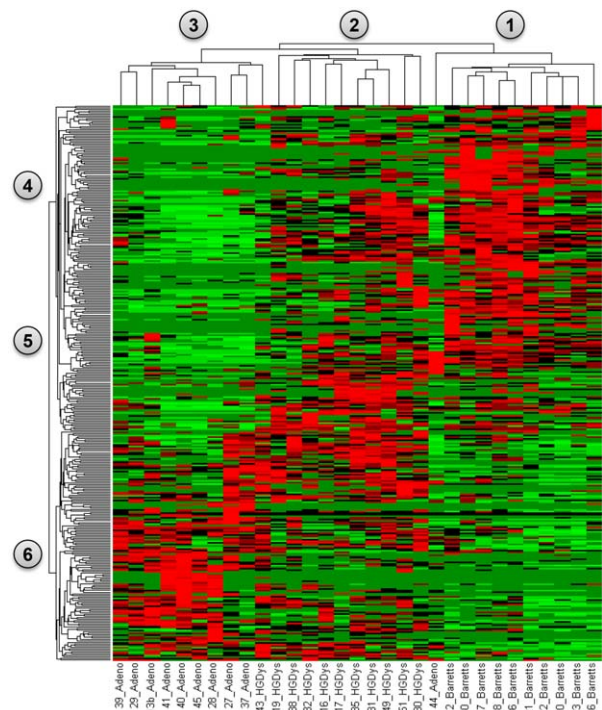


Figure 2. This is a heat-map representation from a supervised cluster analysis of significantly differentially abundant proteins that were identified from Barrett esophagus (Barretts) in column grouping 1 (n=10), high-grade dysplasia (HGDys) in column grouping 2 (n=11), and esophageal adenocarcinoma (Adeno) tissues in column grouping 3 (n=10). Individually significant proteins are represented in row groups 4, 5, and 6. The abundance of each protein is plotted as the mean observed spectral count for each tissue type, where red represents proteins with a normalized spectral count value >1.5 , and green represents those with values <1.5 . Significance was determined using the Kruskal-Wallis test. The results demonstrate clear patterns of protein abundance that can be observed correlating with Barrett esophagus (nodes 1 and 4), high-grade dysplasia (nodes 2 and 5,) and esophageal adenocarcinoma (nodes 3 and 6).

rum discovery set, concentrations of all biomarkers were significantly higher in the EAC patients' samples from the serum validation set with the exception of resistin (Fig. 3).

Final Rule Model

The rule model that was obtained by applying BRL to the merged discovery and validation ELISA data sets is illustrated visually in Figure 4. In the tree, the interior nodes (indicated by ellipses) represent predictor biomarkers; the leaf nodes (indicated by rectangles) represent the patient counts for the number of EAC cases and controls, respectively; and the labels on the arcs represent the serum biomarker levels. The rules, which consist of combinations of individual biomarkers at specific cutoff concentrations

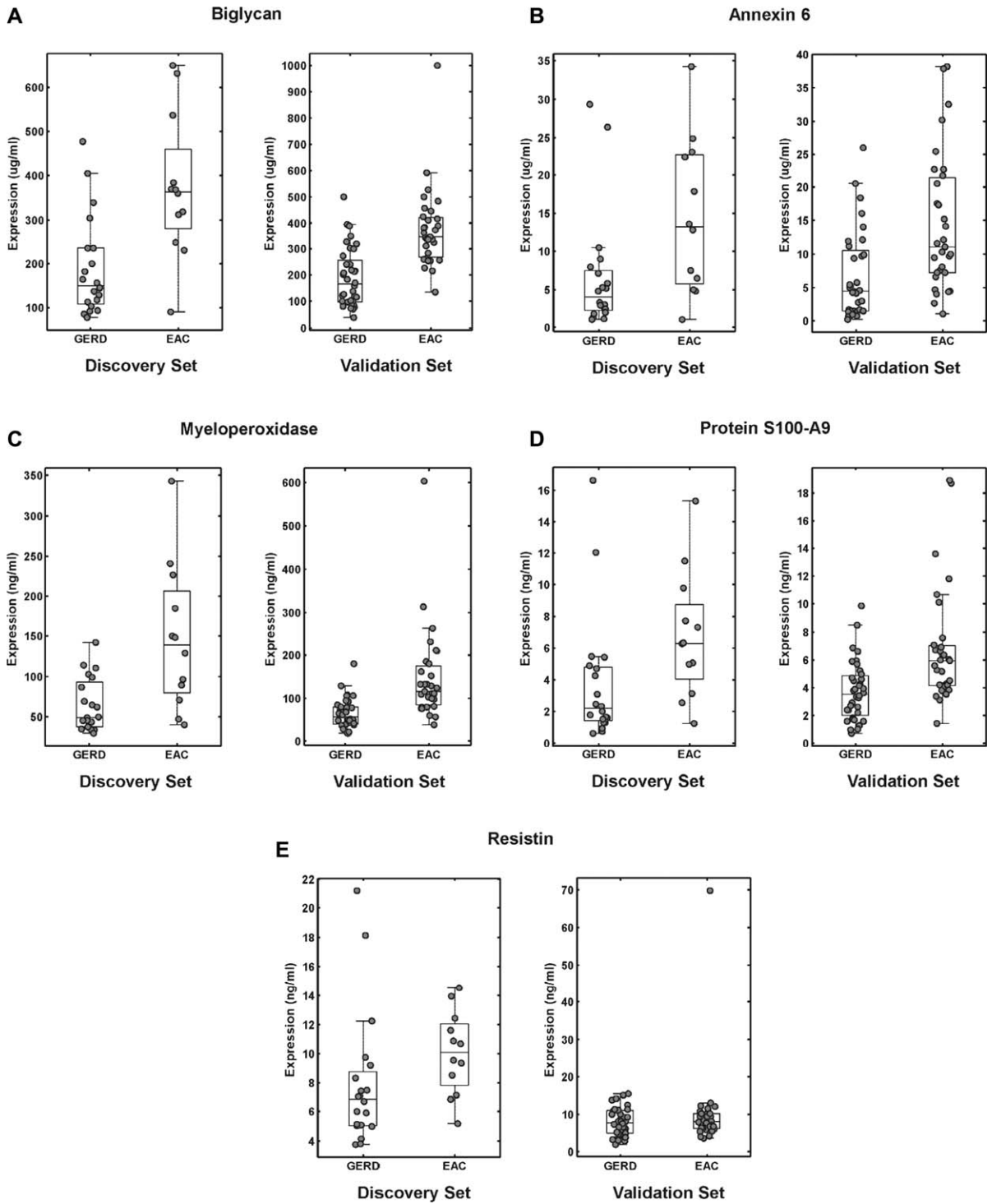


Figure 3. (A-E) Box plots illustrate the distribution and abundance of candidate proteins in serum samples from patients with esophageal adenocarcinoma (EAC) versus gastroesophageal reflux disease (GERD) using enzyme-linked immunosorbent assays. Scatter plots are overlaid on top of the box plots to visualize the individual data points (annexin-A6, dilution factor [df]=1600×; biglycan, df=200×; protein S100-A9, df=25×; myeloperoxidase, df=10×; and resistin, df=5×). For each candidate serum biomarker, the left box presents results from the discovery set, which consisted of 20 GERD samples and 12 EAC samples; and the right box presents results from the validation set, which consisted of 36 GERD samples and 31 EAC samples. The bottom and top horizontal lines delineating each box plot indicate the first and third quartiles of the data, respectively, and the horizontal line inside each box plot indicates the median value. The length of the box plot whiskers is specified as 1.5 times the interquartile range (25th to 75th quartiles) of the data. For the candidate biomarkers, *t* tests were used to compare the mean EAC versus GERD values in each set, and *P* values <.05 were considered significant. The results were significant for all markers except resistin.

TABLE 1. Correlation of Tissue Expression Determined by Liquid Chromatography-Tandem Mass Spectrometry and Spectral Counting With Serum Abundance by Enzyme-Linked Immunosorbent Assay for the Final 5 Candidate Protein Biomarkers^a

Protein	Serum Results: Unnormalized Mean				Tissue Results: Mean Spectral Counts			
	GERD	EAC	<i>P</i>		BE	HGD	EAC	<i>P</i>
			<i>T</i> test	Rank				
Myeloperoxidase, ng/mL	64.36	147.23	.00073	.00256	0.1	3.18	7.7	.01257
Resistin, ng/mL	7.93	10.05	.15967	.01852	0	0	0.8	.0094
Protein S100-A9, ng/mL	3.74	6.77	.04708	.00964	4	6.36	12.2	.03244
Biglycan, µg/mL	190.11	375.24	.00065	.00256	0	0.36	1.1	.01151
Annexin, A6 µg/mL	6.64	14.48	.01956	.02278	0.7	1.45	6.4	.00265

Abbreviations: BE, Barrett esophagus; EAC, esophageal adenocarcinoma; GERD, gastroesophageal reflux disease; HGD, high-grade dysplasia; LC-MS/MS, liquid chromatography-tandem mass spectrometry.

^aThese are results from the up-regulated proteins in Figure 2 represented by red signals in group 6.

produced by BRL, are provided in Table 2. Each rule has a posterior probability associated with it, along with the *P* value obtained from Fisher exact tests.^{13,16} The Fisher exact test is applicable to situations in which the number of samples is fairly small, as in our case, which leads to

small numbers of counts for positive results covered by a rule. The numbers of true-positive results and false-positive results covered by the rule also are presented. This set of rules constitutes the predictive model that can be applied to a future patient for whom these serum

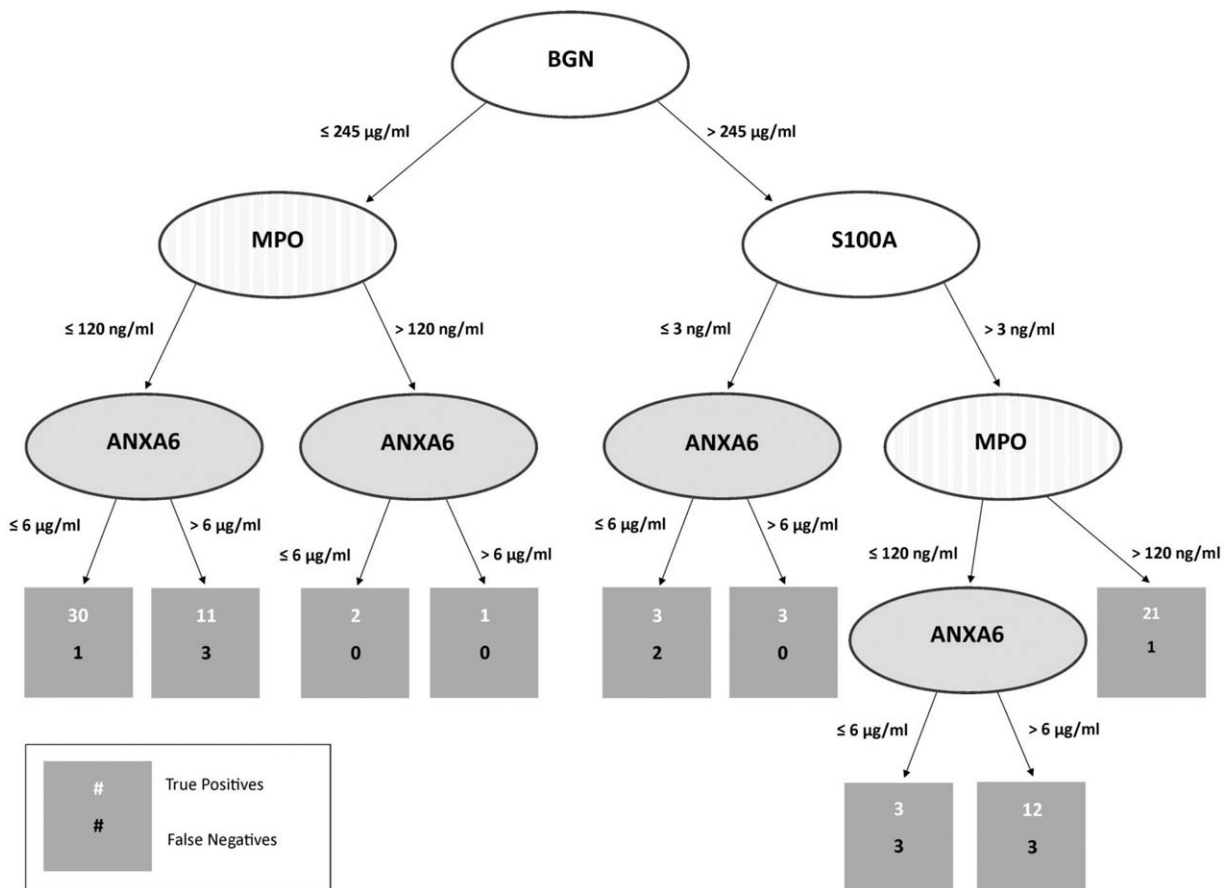


Figure 4. This is a visual representation of the final Bayesian rule-learning model derived from the merged serum enzyme-linked immunosorbent assay data. BGN indicates biglycan; MPO, myeloperoxidase; S100A, protein S100-A9; ANXA6, annexin-A6.

TABLE 2. Rules for the Final Model Using Combinations of Individual Biomarkers at Specific Cutoff Concentrations Produced by Bayesian Rule Learning^a

1. IF (BGN \leq 245 μ g/mL) & (MPO \leq 120 ng/mL) & (ANXA6 \leq 6 μ g/mL) THEN (class=normal) Posterior probability=.939 $P=0$ TP=30 FP=1
2. IF (BGN \leq 245 μ g/mL) & (MPO \leq 120 ng/mL) & (ANXA6 $>$ 6 μ g/mL) THEN (class=normal) Posterior probability=.75 $P=.064$ TP=11 FP=3
3. IF (BGN \leq 245 μ g/mL) & (MPO $>$ 120 ng/mL) & (ANXA6 \leq 6 μ g/mL) THEN (class=normal) Posterior probability=.75 $P=.317$ TP=2 FP=0
4. IF (BGN \leq 245 μ g/mL) & (MPO $>$ 120 ng/mL) & (ANXA6 $>$ 6 μ g/mL) THEN (class=cancer) Posterior probability=.667 $P=.434$ TP=1 FP=0
5. IF (BGN $>$ 245 μ g/mL) & (S100A9 \leq 3 ng/mL) & (ANXA6 \leq 6 μ g/mL) THEN (class=normal) Posterior probability=.571 $P=.624$ TP=3 FP=2
6. IF (BGN $>$ 245 μ g/mL) & (S100A9 \leq 3 ng/mL) & (ANXA6 $>$ 6 μ g/mL) THEN (class=normal) Posterior probability=.8 $P=.177$ TP=3 FP=0
7. IF (BGN $>$ 245 μ g/mL) & (S100A9 $>$ 3 ng/mL) & (MPO \leq 120 ng/mL) & (ANXA6 \leq 6 μ g/mL) THEN (class=normal) Posterior Probability=.5 $P=.777$ TP=3 FP=3
8. IF (BGN $>$ 245 μ g/mL) & (S100A9 $>$ 3 ng/mL) & (MPO \leq 120 ng/mL) & (ANXA6 $>$ 6 μ g/mL) THEN (class=cancer) Posterior probability=.765 $P=.002$ TP=12 FP=3
9. IF (BGN $>$ 245 μ g/mL) & (S100A9 $>$ 3 ng/mL) & (MPO $>$ 120 ng/mL) THEN (class=cancer) Posterior probability=.917 $P=0$ TP=21 FP=1

Abbreviations: ANXA6, annexin-A6; BGN, biglycan; FP, false-positive; MPO, myeloperoxidase; S100A9, protein S100-A9; TP, true-positive.

^aThe 4 serum protein biomarkers used were S100A9, ANXA6, BGN, and MPO.

biomarker levels have been measured, and our objective is to use the matching rule from among this set of mutually exclusive and exhaustive rules to provide an estimate of the probability that the patient has EAC.

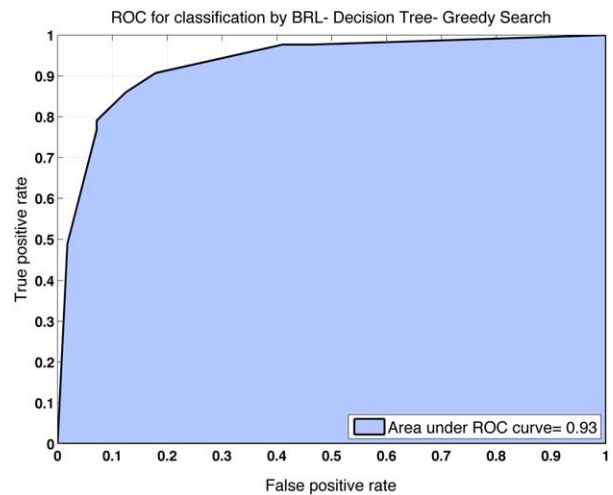


Figure 5. This receiver operating characteristic curve (ROC) was generated from 10-fold cross-fold validation on the merged data sets to estimate the classification performance of the final Bayesian rule-learning (BRL) predictive model.

Evaluation of Alternative Rule Models

The highest accuracy that we obtained when a BRL predictive model was learned using the discovery data set and then applied to the validation data set was 76%, with a BACC of 74% and an AUROC of 86%. The highest accuracy that we obtained when a BRL predictive model was learned using the validation data set and then applied to the discovery data set was 75%, with a BACC of 73% and an AUROC of 84%.

These 2 reciprocal results indicate that BRL is accurate for modeling the uncertainty in the validity of the rule models because of the similar results obtained in the 2 independent data sets for EAC classification. The cross-validation results for the merged discovery and validation data sets analyzed by BRL yielded an overall accuracy of 87%, a BACC of 86%, and an AUROC of 93% (Fig. 5).

DISCUSSION

Serum biomarkers hold significant promise for the early, noninvasive detection of EAC. However, direct identification of novel biomarkers from serum presents a challenging analytical problem because of the very high dynamic range of protein concentrations present in the complex serum proteome.²² Therefore, in the current study, we used an LC-MS/MS-based tissue proteomics discovery approach to guide the selection of candidate serum biomarkers that were significantly and differentially abundant in the tissue samples along the disease progression pathway from BE to EAC and that had clinical and functional relevance.

These results demonstrate that the observed differences in abundance of the selected proteins along the BE-HGD-EAC disease spectrum in FFPE-derived tissue samples were mirrored by the corresponding protein biomarker concentrations in the corresponding serum samples, as summarized in Table 1. The tissue-based results were used to guide targeted, serum-based biomarker discovery; and, with the ease of serum sample collection and relatively low cost, our B-AMP panel and rule model were able to identify patients with EAC with an overall accuracy of 87%. It is noteworthy that, although we originally identified 5 elevated biomarkers, including resistin, the final BRL model excluded it, because resistin does not appear to add any predictive value to the best scoring models based on the other 4 biomarkers.

Over the years, several biologic, immunohistochemistry-based, and transcriptomic tissue-based analyses have been used to identify biomarkers of neoplastic progression in patients with BE. Thus, as expected, there are many reports citing aberrant biologic processes that occur in the development of EAC, such as cell cycle abnormalities and numerous genetic and epigenetic alterations, including loss of heterozygosity, polyploidy, and aneuploidy. Although proteins such as tumor protein TP53 (p53),^{23,24} β -catenin (CTNNB1),²⁵ p16,^{24,26} and cyclin D1 (CCND1)²⁷ have been studied as potential tissue-based immunohistochemical biomarkers of progression,²⁸ none have resulted in widespread clinical adoption or have demonstrated adequate clinical utility, probably because of the genetic heterogeneity of EAC between patients. On the basis of these results, it is apparent that a multiple protein panel approach combined with mathematical modeling may offset some of the poor sensitivity associated with a single biomarker “up” or “down” approach.

With respect to the biomarkers identified in our panel, the prognostic significance of BGN (an extracellular matrix component with a known role in epithelial-to-mesenchymal transdifferentiation central to BE carcinogenesis), ANXA6 (which belongs to the annexin family of calcium and phospholipid binding proteins and is a motility-promoting factor), MPO (an oxidant-generating enzyme linked to cancer progression), and S100A9 (which promotes tumor growth in inflammation-associated cancer development) has been noted in several tumor types, including esophageal squamous cell carcinoma.²⁹⁻³³

EAC is a genetically and phenotypically heterogeneous malignancy, as described above, and we certainly would be cautious in claiming that these 4 biomarkers will capture all EACs, although the classification performance

of the panel in our 2 clinically independent patient groups suggests that it captures the majority of these cancers, representing the downstream protein expression patterns of the common upstream genetic changes that alter these key pathways. However, published studies focused on serum protein biomarkers of EAC are limited to an early report of elevated levels of the squamous cell carcinoma antigen (SCC), carcinoembryonic antigen, and cytokeratin 19-fragment (CYFRA 21-1) in patients with advanced esophageal cancer³⁴ and more recent evaluations of the circulating lymphocyte antigen 6 complex locus K (LY6K) and elevated serum levels of serum gastrin in patients with a diagnosis of HGD or EAC.^{35,36}

Similar to our study, tissue-based and serum-based protein discovery and proteomic studies have been reported. A 2007 comparative mass spectrometry proteomics analysis identified candidate tissue proteins in surgical specimens that, by hierarchical clustering analysis, accurately discriminated BE and EAC and identified 38 differentially abundant proteins, among which Rho guanosine diphosphate (GDP) dissociation inhibitor 2, α -enolase, lamin A/C, elongation factor Tu, thioredoxin domain-containing protein 17, and nucleoside-diphosphate kinase A had up-regulated expression levels of both messenger RNA and protein EAC compared with BE.³⁷ Several of the those proteins or their isoforms, along with previously reported progression-related proteins, also were differentially abundant in our tissue discovery data set, including CTNNB1, Rho GDP dissociation inhibitor 2, elongation factor Tu, and thioredoxin domain-containing protein 17. In a very recent methods publication, as noted in our study, tissue-based studies also have been extended to demonstrate the feasibility of using LCM and LC-MS/MS analysis of esophageal tissue biopsy specimens for robust proteomic analysis.³⁸

The main weakness of our current study is the small numbers of samples available for EAC case-control discrimination. However, we were able to demonstrate the ability of rule-learning methods to successfully predict class values accurately using 2 independent data sets with similar distributions of cases and controls. We present a predictive model learned from the merged data set that needs to be validated in a larger prospective patient cohort.

Thus, the next logical steps would be to evaluate the classification performance our B-AMP serum biomarker panel in other, larger, recently reported case-control patient groups and to test it prospectively to detect and/or monitor progression of EAC. This evaluation follow-up study would necessarily include the measurement of the

levels of these serum biomarkers in samples from patients with other solid organ epithelial malignancies as well as clinically relevant nonmalignant conditions to evaluate EAC specificity.

The application of serum-based proteomic biomarker panels and risk-prediction models like ours could be extended to other studies to help determine the presence or absence of BE, HGD, or EAC. Potential advantages would include: 1) improved use of clinical resources using blood-based detection as a means of directing effective screening and post-therapy surveillance; 2) detecting progression from BE to HGD or EAC in patients undergoing surveillance; 3) preventing deaths from EAC using an assay in high-risk patients to identify BE, HGD, and EAC; 4) tracking therapeutic responses, thereby enabling tailored therapy based on individual disease biology; and 5) detecting subclinical EAC recurrence before the development of recurrence as detected by clinical imaging.

FUNDING SUPPORT

This work was supported in part by awards P30CA047904 and R01-LM010950 from National Institutes of Health, and by the David E. Gold & Irene Blumenkranz Foundation, and by the David Scaife Foundation.

CONFLICT OF INTEREST DISCLOSURES

A provisional patent application has been filed by the University of Pittsburg for Drs. Zaidi, Jobe, Zeng, Balasubramanian, Gopalakrishnan, and Bigbee as inventors of "Serum Biomarker Panel for the Detection of Esophageal Adenocarcinoma" (US Provisional Patent Application no. 61/922,665; December 31, 2013).

REFERENCES

- Dubecz A, Solymosi N, Stadlhuber RJ, Schweigert M, Stein HJ, Peters JH. Does the incidence of adenocarcinoma of the esophagus and gastric cardia continue to rise in the twenty-first century? A SEER database analysis [published online ahead of print November 15, 2013]. *J Gastrointest Surg*. 2013.
- Prasad GA, Bansal A, Sharma P, Wang KK. Predictors of progression in Barrett's esophagus: current knowledge and future directions. *Am J Gastroenterol*. 2010;105:1490-1502.
- Zhang Y. Epidemiology of esophageal cancer. *World J Gastroenterol*. 2013;19:5598-5606.
- Spechler SJ. Barrett esophagus and risk of esophageal cancer: a clinical review. *JAMA*. 2013;310:627-636.
- Spechler SJ. Screening and surveillance for complications related to gastroesophageal reflux disease. *Am J Med*. 2001;111(suppl 8A):130S-136S.
- Sampliner RE. Practice guidelines on the diagnosis, surveillance, and therapy of Barrett's esophagus. The Practice Parameters Committee of the American College of Gastroenterology. *Am J Gastroenterol*. 1998;93:1028-1032.
- Sampliner RE; Practice Parameters Committee of the American College of Gastroenterology. Updated guidelines for the diagnosis, surveillance, and therapy of Barrett's esophagus. *Am J Gastroenterol*. 2002;97:1888-1895.
- Conio M, Cameron AJ, Romero Y, et al. Secular trends in the epidemiology and outcome of Barrett's esophagus in Olmsted County, Minnesota. *Gut*. 2001;48:304-309.
- Reavis KM, Morris CD, Gopal DV, Hunter JG, Jobe BA. Laryngopharyngeal reflux symptoms better predict the presence of esophageal adenocarcinoma than typical gastroesophageal reflux symptoms. *Ann Surg*. 2004;239:849-856; discussion 856-858.
- Reid BJ, Prevo LJ, Galipeau PC, et al. Predictors of progression in Barrett's esophagus II: baseline 17p (p53) loss of heterozygosity identifies a patient subset at increased risk for neoplastic progression. *Am J Gastroenterol*. 2001;96:2839-2848.
- Elias JE, Gygi SP. Target-decoy search strategy for increased confidence in large-scale protein identifications by mass spectrometry. *Nat Methods*. 2007;4:207-214.
- Teng PN, Rungruang BJ, Hood BL, et al. Assessment of buffer systems for harvesting proteins from tissue interstitial fluid for proteomic analysis. *J Proteome Res*. 2010;9:4161-4169.
- Gopalakrishnan V, Lustgarten JL, Visweswaran S, Cooper GF. Bayesian rule learning for biomedical data mining. *Bioinformatics*. 2010;26:668-675.
- Ryberg H, An J, Darko S, et al. Discovery and verification of amyotrophic lateral sclerosis biomarkers by proteomics. *Muscle Nerve*. 2010;42:104-111.
- Bigbee WL, Gopalakrishnan V, Weissfeld JL, et al. A multiplexed serum biomarker immunoassay panel discriminates clinical lung cancer patients from high-risk individuals found to be cancer-free by CT screening. *J Thorac Oncol*. 2012;7:698-708.
- Sokal RR, Rohlf FJ. *Biometry: The Principles and Practice of Statistics in Biological Research*. New York: WH Freeman; 1995.
- Neapolitan RE. *Learning Bayesian Networks*. Upper Saddle River, NJ: Prentice Hall; 2004.
- Cooper GF, Herskovits E. A Bayesian method for the induction of probabilistic networks from data. *Machine Learning*. 1992;9:309-347.
- Lustgarten JL. *A Bayesian Rule Generation Framework for "Omic" Biomedical Data Analysis*. Pittsburgh, PA: University of Pittsburgh; 2009.
- Lustgarten JL, Visweswaran S, Gopalakrishnan V, Cooper GF. Application of an efficient Bayesian discretization method to biomedical data. *BMC Bioinformatics*. 2011;12:309.
- Lustgarten JL, Visweswaran S, Grover H, Gopalakrishnan V. An evaluation of discretization methods for learning rules from biomedical datasets. In: Doble M, ed. *International Conference on Bioinformatics, Computational Biology, Genomics and Chemoinformatics (BCBGC-08)*. International Society for Research and Technology/Curran Associates, Inc. (Proceedings.com); 2008:527-532.
- Anderson NL, Anderson NG. The human plasma proteome: history, character, and diagnostic prospects. *Mol Cell Proteomics*. 2002;1:845-867.
- Ramel S, Reid BJ, Sanchez CA, et al. Evaluation of p53 protein expression in Barrett's esophagus by two-parameter flow cytometry. *Gastroenterology*. 1992;102(4 pt 1):1220-1228.
- van Dekken H, Hop WC, Tilanus HW, et al. Immunohistochemical evaluation of a panel of tumor cell markers during malignant progression in Barrett esophagus. *Am J Clin Pathol*. 2008;130:745-753.
- Washington K, Chiappori A, Hamilton K, et al. Expression of beta-catenin, alpha-catenin, and E-cadherin in Barrett's esophagus and esophageal adenocarcinomas. *Mod Pathol*. 1998;11:805-813.
- Barrett MT, Sanchez CA, Galipeau PC, Neshat K, Emond M, Reid BJ. Allelic loss of 9p21 and mutation of the CDKN2/p16 gene develop as early lesions during neoplastic progression in Barrett's esophagus. *Oncogene*. 1996;13:1867-1873.
- Bani-Hani K, Martin IG, Hardie LJ, et al. Prospective study of cyclin D1 overexpression in Barrett's esophagus: association with increased risk of adenocarcinoma. *J Natl Cancer Inst*. 2000;92:1316-1321.
- Ong CA, Lao-Sirieix P, Fitzgerald RC. Biomarkers in Barrett's esophagus and esophageal adenocarcinoma: predictors of progression and prognosis. *World J Gastroenterol*. 2010;16:5669-5681.
- Castillo-Tong DC, Pils D, Heinze G, et al. Association of myeloperoxidase with ovarian cancer. *Tumour Biol*. 2014;35:141-148.
- Fan NJ, Gao CF, Wang CS, et al. Identification of the up-regulation of TP-alpha, collagen alpha-1(VI) chain, and S100A9 in esophageal squamous cell carcinoma by a proteomic method. *J Proteomics*. 2012;75:3977-3986.

31. Zhu YH, Yang F, Zhang SS, Zeng TT, Xie X, Guan XY. High expression of biglycan is associated with poor prognosis in patients with esophageal squamous cell carcinoma. *Int J Clin Exp Pathol.* 2013;6:2497-2505.
32. Lomnyska MI, Becker S, Bodin I, et al. Differential expression of ANXA6, HSP27, PRDX2, NCF2, and TPM4 during uterine cervix carcinogenesis: diagnostic and prognostic value. *Br J Cancer.* 2011;104:110-119.
33. Sakwe AM, Koumangoye R, Guillory B, Ochieng J. Annexin A6 contributes to the invasiveness of breast carcinoma cells by influencing the organization and localization of functional focal adhesions. *Exp Cell Res.* 2011;317:823-837.
34. Kawaguchi H, Ohno S, Miyazaki M, et al. CYFRA 21-1 determination in patients with esophageal squamous cell carcinoma: clinical utility for detection of recurrences. *Cancer.* 2000;89:1413-1417.
35. Ishikawa N, Takano A, Yasui W, et al. Cancer-testis antigen lymphocyte antigen 6 complex locus K is a serologic biomarker and a therapeutic target for lung and esophageal carcinomas. *Cancer Res.* 2007;67:11601-11611.
36. Wang JS, Varro A, Lightdale CJ, et al. Elevated serum gastrin is associated with a history of advanced neoplasia in Barrett's esophagus. *Am J Gastroenterol.* 2010;105:1039-1045.
37. Zhao J, Chang AC, Li C, et al. Comparative proteomics analysis of Barrett metaplasia and esophageal adenocarcinoma using two-dimensional liquid mass mapping. *Mol Cell Proteomics.* 2007;6:987-999.
38. Stingl C, van Vilsteren FG, Guzel C, et al. Reproducibility of protein identification of selected cell types in Barrett's esophagus analyzed by combining laser-capture microdissection and mass spectrometry. *J Proteome Res.* 2011;10:288-298.